Applied Energy 248 (2019) 162–173

Contents lists available at ScienceDirect

Applied Energy

journal homepage: www.elsevier.com/locate/apenergy

A spectral splitting solar concentrator for cascading solar energy utilization by integrating photovoltaics and solar thermal fuel

Wanjun Qu, Hui Hong*, Hongguang Jin

Institute of Engineering Thermophysics, Chinese Academy of Sciences, Beijing 100190, China
University of Chinese Academy of Sciences, Beijing 100049, China

HIGHLIGHTS

- A spectral splitting concentrator is proposed and designed for cascading radiation.
- Full-spectrum radiation is selectively cast to photovoltaics and solar reactor.
- "Solar thermal" energy does not participate in the photovoltaic heat generation.
- Uniform solar flux distribution is offered over the photovoltaics and solar reactor.
- 5% absolute enhancement of solar conversion is realized by the designed concentrator.

ARTICLE INFO

Keywords:
Cascading solar energy utilization
Concentrating solar photovoltaic/thermochemical hybrid system
Spectral splitting concentrator
Solar radiation distribution

ABSTRACT

Full-spectrum solar energy utilization has drawn widespread attention for cascading solar energy utilization. The hybrid approach integrating photovoltaic generation and solar thermochemical reaction is attractive to convert full-spectrum solar energy into electricity and chemical energy. This paper proposes a concentrating solar photovoltaic/thermochemical hybrid system. Meanwhile, a spectral splitting concentrator is proposed and designed. The proposed concentrator consists of above-mirror and sub-mirror. The above-mirror enables the visible spectrum to be concentrated onto photovoltaics. The sub-mirror allows the infrared and ultraviolet spectra to be concentrated onto a solar thermochemical reactor. The design methodology based on ray tracing is described. The distribution of solar radiation on the photovoltaics and the thermochemical reactor is made analysis. The results show that solar radiation can be uniformly cast to the photovoltaic surface without using secondary optical element; the common solar flux concentration of thermochemical reactor is also mitigated. The proposed spectral splitting concentrator is introduced in the hybrid system. The total conversion efficiency of the solar energy can exceed 20%. Compared with individual photovoltaic electricity and solar thermal fuel, this hybrid system has the potential to increase the conversion efficiency of solar energy into both electricity and fuel, with greater than 5% absolute enhancement. The design of the spectral splitting concentrator provides the possibility of cascading utilization of full-spectrum solar energy.

1. Introduction

Solar energy as the largest renewable energy is expected to replace fossil fuel for satisfying the energy demand of humankind, which provides access to reliable and ample supplies of energy [1]. At present, full-spectrum solar energy utilization has attracted widespread attention [2]. For example, various approaches [3] and experiments [4] have been proposed and conducted to improve full-spectrum solar energy utilization; US Department of Energy has put forward a research plan of full-spectrum solar energy utilization in 2013 [5].

According to the spectral response characteristic [6], the full-spectrum solar radiation could be converted into photovoltaic electricity (using visible spectrum) and solar heat (using ultraviolet and infrared spectra). Correspondingly, the hybridization of solar photovoltaic (PV) and solar thermal processes is common considered to improve full-spectrum solar energy utilization. The waste heat recovery hybrid system and spectral splitting hybrid system are two typical hybridizing approaches. It is based on whether the ultraviolet and infrared spectra directly participate in photovoltaic heat generation.

Waste heat recovery hybrid system: Full-spectrum solar radiation is

* Corresponding author at: Institute of Engineering Thermophysics, Chinese Academy of Sciences, Beijing 100190, China.
E-mail address: honghui@iet.cn (H. Hong).

https://doi.org/10.1016/j.apenergy.2019.04.115
Received 14 January 2019; Received in revised form 26 March 2019; Accepted 16 April 2019

first concentrated onto photovoltaics and then converted into photovoltaic electricity and waste heat of the photovoltaics. This dissipated heat of a photovoltaics can be further used in heating, cooling and other heating related applications for domestic and industrial processes. For example, Carlo Renno [7] proposed a concentrating solar photovoltaic/thermal hybrid system (CPV/T) with waste heat recovery, it was satisfied for the thermal demand of a building space by recovering the photovoltaic heat. Similarly, Coventry et al. [8] designed and fabricated a test bench about CPV/T, the measured results show that the 58% low-temperature waste heat from photovoltaics can be recovered to produce domestic hot water. The total efficiency of solar energy utilization can exceed 50% in this type of hybrid system.

From the viewpoint of thermodynamics, the waste heat at below 60 °C belongs to low-grade energy in most CPV/T. Thus, to output more high-grade energy, the Organic Rankine Cycle (ORC) is adopted to further convert waste heat into work. For example, Tourkov et al. [9] studied the effect of different working fluids of the ORC on the performance of its expander and the efficiency of solar energy conversion. By using alkanes as working fluid, ORC had the highest performance of photovoltaic heat into work. The solar energy efficiency of hybrid system can excess 20%, and it was higher than that of the individual PV system. Rahbar, et al. [10] established a 1-D modeling to investigate the solar energy efficiency of the CPV/T integrating with ORC. The results showed that the solar energy efficiency was about 18%, in which the contribution of ORC was about 6 percent.

Spectral splitting hybrid system: To realize a desired solar energy efficiency, up to now, various spectral splitting approaches have been proposed and adopted [11]. The incident solar radiation can be split into ultraviolet, visible and infrared spectra. The split visible spectrum belonging to the "solar photovoltaic" spectral band can be used to produce electricity. The split ultraviolet and infrared spectra as "solar thermal" spectral band does not yet participate in the low-grade photovoltaic heat generation. On the contrary, the solar energy from these high-grade spectral bands is directly converted into solar heat at medium-high temperature and chemical energy.

Important progress had been made in the development of spectral splitting hybrid systems [12]. For example, Ulavi et al. [13] proposed a non-tracking hybrid system that can be envisioned as an add-on to an existing roof-top PV installation. By using a wavelength selective film, the ultraviolet and infrared portion of the spectrum was reflected towards a tubular absorber, and the visible spectrum was transmitted to the PV. The hybrid system can provide 20% more energy compared with a single system at the same area. Jiang et al. [14] described a two-stage parabolic trough hybrid system. A spectral beam splitting filter was positioned between the tubular receiver and the concentrator to achieve a better spectral match between the received sunlight and the photovoltaics. The full-spectrum energy was eventually converted into photovoltaic electricity and solar heat (in the range of 250–300 °C). This hybrid system can reduce the heat load of the CPV by 20.7% and enhance the working potential of the solar heat from the conversion of "solar thermal" radiation. Similarly, Segal et al. [15] integrated a spectral beam splitting filter with a normal solar tower system, the temperature of solar heat can be further enhanced.

Another more attractive approach involves synergistically hybridizing the concentrating solar photovoltaic process with the solar chemical process. Here, the concentrating solar photovoltaic process is known as photovoltaic power generation under the concentrating sunlight condition [16]. The solar chemical process mainly includes solar photochemical process and solar thermochemical process. The solar photochemical process [17] describes a chemical reaction caused by direct absorption of ultraviolet, visible and infrared radiation and the product of solar energy is called as solar fuel. The solar thermochemical process makes use of concentrated solar heat radiation as the energy source to drive endothermic reactions, in which solar energy is converted into fuel called as solar thermal fuel [18]. In this paper, the methanol decomposition is considered and adopted which operates at low/medium temperature.

In contrast to the conversion of solar radiation into solar heat, the "solar thermal" spectral energy was directly converted into the chemical energy of solar fuel. Bicer et al. [19] constructed an experiment setup with a spectrum splitting mirror. The ultraviolet radiation was split from the incident full-spectrum radiation and was used in the photonic hydrogen process. As a result, this part of ultraviolet spectral energy was converted into high-grade chemical energy of solar fuel, rather than 250–300 °C solar heat. As indicated in some works [20,21], the mid-temperature (less than 300 °C) thermochemical reaction can participate in the full-spectrum solar energy conversion. Furthermore, our previous work had proposed an innovational concentrating solar photovoltaic/ thermochemical hybrid system [22]. The infrared spectrum penetrated through the transparent PV and directly drove a methanol decomposition reaction. The total conversion efficiency of solar energy to both electricity and chemical energy of solar thermal fuel can reach approximately 55%.

In the spectral splitting hybrid system, it is an important factor for photovoltaic panel to hold homogenous solar flux distribution [23]. It is because that a non-uniform illumination over the photovoltaics would bring about undesired temperature peak and current mismatch in the inner of photovoltaics. This non-uniform illumination situation would impact the photovoltaic performance and limit the photovoltaic lifetime. It is a challenge that the uniform illumination influences the solar energy conversion [24].

Homogenization of the solar flux: A refractor or reflector (called as secondary optics) is added in front of the photovoltaics. The incident sunlight is first concentrated on the secondary optics, and the path of the sunlight can be bended subsequently when the sunlight penetrates through a refractor or is reflected by a reflector. In this manner, the previous focus profile of a Gaussian distribution on the photovoltaics can be improved to a relatively homogenous distribution [25]. For the refractor, the common types include kaleidoscope, half egg and some compound form [26], which are generally adopted in the point focus and shown in Appendix A. For the reflector, the common types are inverted truncated pyramid in the point focus or compound parabolic concentrator (CPC) in the line focus [27]. The tests show that adopting secondary optics can provide a good homogenization of the solar radiation onto the CPV, thereby enabling the CPV to obtain a high-efficiency performance. Note that the refractor has the problem of chromatic aberration that is related to the photovoltaic power drop [28]. In addition, both a refractor and a reflector can cause additional optical loss in the homogenizing sunlight process. For this reason, designing concentrator has been paid attention to offer a uniform illumination over the photovoltaics, rather than adding a secondary optics.

Two main pathways were considered, including the redesign of a mature concentrator and the implementation of a multi-faceted concentrator. Regarding the former pathway, a new profile of a concentrator was analytically derived by the geometrical reverse design method. For example, Bader et al. [29] tailored a normal parabolic trough concentrator when an initial source-target map of the CPV was given. Moreover, they studied the effect of sun shape and mirror imperfections on the irradiation uniformity. Their results showed that the local Gaussian distribution on the photovoltaic panel can be moderated. Nilsson et al. [30] introduced three parabolic solar concentrators with different structures. By breaking the symmetry, the proposed structures can reduce the peak irradiation over the photovoltaics. Zhuang et al. [31] presented a novel hybrid Fresnel-based concentrator, by optimizing the prism displacement, the spatial non-uniformity on the photovoltaic surface can be reduced to less than 16.2%. It can be considered as a practical concentrator in the point focus.

The multi-faceted concentrators can also provide homogenous irradiation for CPV [32]. Its homogenous irradiation process is implemented by superimposing each focus spot of every facet or moving the photovoltaic panel from the focus plane. This type of concentrator [33] is usually an analogous disk comprised by an array of spherical

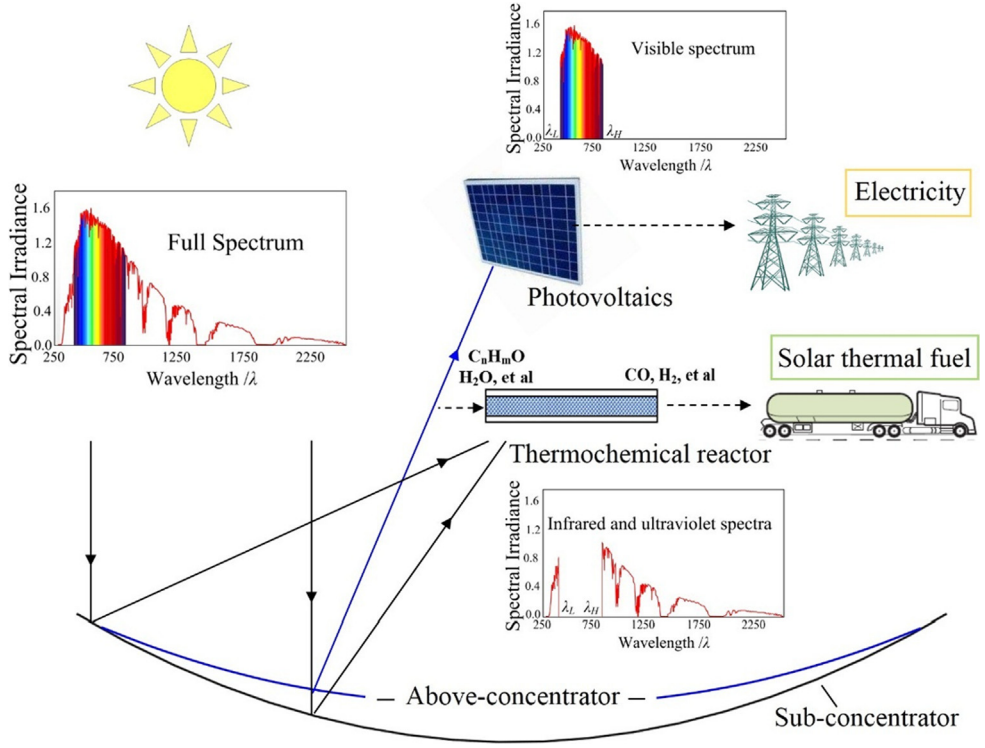

Fig. 1. Schematic diagram of cascading solar energy utilization: visible spectrum is converted into electricity by photovoltaics; infrared and ultraviolet spectra are used to produce solar thermal fuel.

mirrors. The feasibility of such a concentrator has been demonstrated by Ricardo [34] in a test bench. Compared to the analogous disk, the Fresnel mirrors have notable advantage, in which the focus spot formed is in the form of a belt. Such a belt of illumination can be superimposed together with other belts over the surface of CPV, resulting in a uniform distribution of solar flux. [35]

In this paper, a spectral splitting parabolic trough concentrator having an above-mirror and a sub-mirror is proposed. The design methodology is described below. The effects of geometric relationship between the above-mirror and the sub-mirror on the photovoltaic concentration ratio are analyzed. The feature is pointed out for the solar flux distribution over the photovoltaics and solar thermochemical reactor. Furthermore, by adopting designed splitting concentrator, a feasible performance of typical concentrating solar photovoltaic/thermochemical hybrid system is achieved.

2. Description of the proposed spectral splitting concentrator

Fig. 1 shows a schematic diagram of the concentrating solar photovoltaic/thermochemical hybrid system. The described spectral splitting concentrator consists of the above-mirror and the sub-mirror. The full-spectrum incident sunlight first reaches the above-mirror. This above-mirror selectively casts the sunlight in the visible spectrum (380–780 nm) onto the photovoltaics for generating electricity. Meanwhile, the sunlight in the ultraviolet and infrared spectra (280–380 nm and 780–4000 nm) can penetrate through the above-mirror. Subsequently, this part of penetrated sunlight is concentrated by the sub-mirror and enters onto the solar thermochemical reactor, in which an endothermic reaction can be conducted. Then, ultraviolet and infrared radiations are converted into chemical energy of solar thermal fuel. The produced photovoltaic electricity and solar thermal fuel can be stored or easily transported to a remote place.

Here, the above-mirror and the sub-mirror are typical parabolic troughs. There exists a layer of wavelength selective film over the above-mirror. By using this selective film, the radiation in the targeted spectrum can be reflected with high reflectance. The rest radiation can penetrate through the above-mirror with high transmittance and reach the sub-mirror. The sub-mirror has an ultrathin silver coating, by this silver coating, all radiations reaching the sub-mirror can be reflected with high reflectance. The relative position between above-mirror and sub-mirror has a crossed point that decides the aperture width of the above-mirror and the trace of the concentrated rays. Here, by adjusting the relative position, the concentrated sunlight from the above-mirror can also be uniformly distributed over the photovoltaics. It is noted that the width of above-mirror is possibly smaller than that of the sub-mirror. In this case, the part of incident sunlight in the full-spectrum would directly reach the surface of sub-mirror and be concentrated onto the solar thermochemical reactor.

The proposed spectral splitting concentrator and hybrid system have the following three distinct features: (1) Spectral splitting concentrator enables incident radiation to be preliminarily split into a photovoltaic band and a thermal band, and then the split solar radiation is further concentrated for cascading solar energy utilization. In contrast, the incident radiation is often first concentrated and then split. From the viewpoint of the irreversibility, if such high-grade concentrated sunlight is split by using a stand-alone spectral splitting filter, there could be serious irreversible loss caused. (2) Spectral splitting concentrator can reduce thermalization and recombination losses of photovoltaics, the overall entropy generation could be minimized. Split solar radiation in the photovoltaic band is often in the visible spectrum, which can match well with photovoltaics and have a higher solar-to-electricity efficiency. Regarding the thermal band, it often includes high-frequency ultraviolet spectrum and low-frequency infrared spectrum. Solar radiation in the thermal band is unsuitable for photovoltaic power generation, thus, is cast to solar thermochemical reactor. Moreover, the homogenization of solar flux can be realized which does not rely on the help of common secondary optical element. (3) Full-spectrum solar energy is converted into high-quality electricity and work-equivalent chemical energy of solar thermal fuel. The proposed hybrid system combines solar photovoltaic process and solar

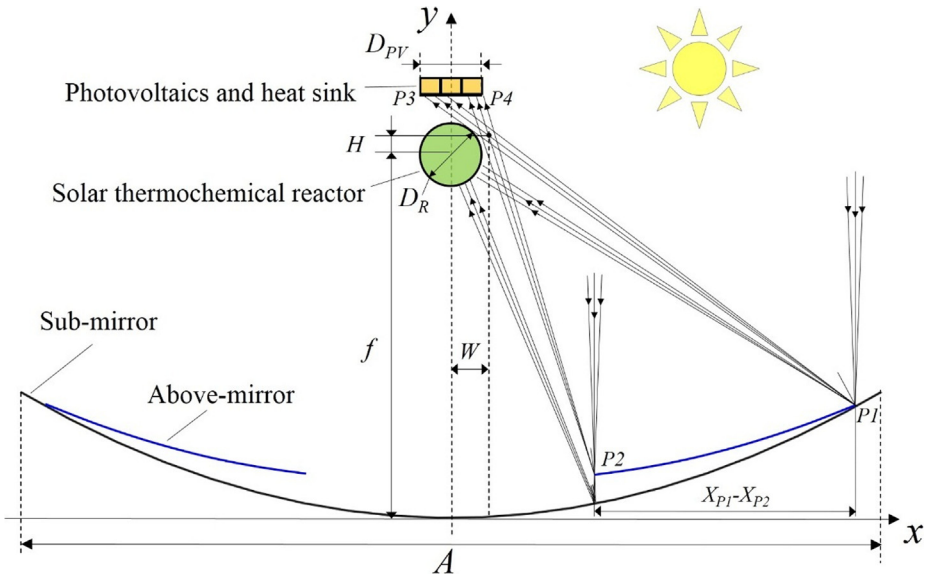

Fig. 2. Geometric ray diagram: the partial of solar radiation is split from full spectrum and concentrated onto photovoltaics by using above-mirror; the rest radiation reaches sub-mirror and is concentrated onto solar thermochemical reactor by using sub-mirror.

thermochemical process. In the former process, the solar radiation in the photovoltaic band is used to excite electrons, and converted into electricity. In the latter process, the solar radiation in the thermal band is used to drive hydrocarbons cracking or reforming, and ultimately exists as a form of chemical energy of solar thermal fuel. This energy conversion path of ultraviolet and infrared spectrum is different from conventional CPV/T where the spectral energy is converted into low-temperature solar heat. These features can provide a possibility to cascading use full-spectrum solar energy.

3. Design methodology

3.1. Geometric parameter

For formulating the physical structure and the ray trace, a Cartesian coordinate is established, as depicted in Fig. 2. The optical axis is along the focus point of the sub-mirror. With regard to this sub-mirror, the profile is a parabolic trough and is expressed as Eq. (1). The parameter f denotes the focus length, and the sunlight can be concentrated by the sub-mirror on the focus position $(0, f)$. Here, by using well-known parabolic trough Eq. (1), the profile function of the above-mirror is determined by vertical and horizontal transformations. Thus, it can be considered that the above-mirror is obtained by a horizontal shift W and vertical shift H of the sub-mirror. The focus length of above-mirror is the same as that of the sub-mirror. At a given W and H, the mathematical expression of the above-mirror is given in Eq. (2).

$$y = x^2/(4 \cdot f) \tag{1}$$

$$y = \begin{cases} (x + W)^2/(4 \cdot f) + H, & x < 0 \\ (x - W)^2/(4 \cdot f) + H, & x > 0 \end{cases} \tag{2}$$

To simplify the complexity of the variables, the focus length f of the sub-mirror is chosen as the characteristic length. The relative shifts of above-mirror to sub-mirror can be further expressed as $Wc = W/f$ and $Hc = H/f$. As a result, the mathematical equations of the two mirrors are rewritten as the following Eqs. (3) and (4):

$$y = x^2/4 \tag{3}$$

$$y = \begin{cases} (x + Wc)^2/4 + Hc, & x < 0 \\ (x - Wc)^2/4 + Hc, & x > 0 \end{cases} \tag{4}$$

In addition, to generally describe this design process, we make other physical parameters to be dimensionless. For example, the aperture width of the sub-mirror, the photovoltaic width and the diameter of thermochemical reactor can be expressed as $Ac = A/f$, $D_{PVC} = D_{PV}/f$ and $D_{RC} = D_R/f$, respectively.

In the optical design process, some boundary conditions are considered between the geometric structure and the concentrated sunlight. (i) The straight-line distance needs to be greater than the thermochemical reactor's radius $D_{RC}/2$, which is between the center point of the thermochemical reactor and the trace of the reflected sunlight from the above-mirror. Satisfying this condition can ensure all sunlight from the above-mirror reaches the photovoltaics rather than the solar thermochemical reactor. (ii) The reflected sunlight *P1P3* from above-mirror is the outmost sunlight in the concentrated sunlight cone of above-mirror. The spot *P1* is the cross point between above-mirror and sub-mirror, and the x-coordinate of spot *P1* is less than $Ac/2$. The spot *P3* locates at the photovoltaic border, and the x-coordinate of spot *P3* equals to $-D_{PVC}/2$. (iii) The reflected sunlight *P2P4* cannot be intercepted by solar thermochemical reactor. The spot *P2* is the inner point of above-mirror, and the spot *P4* locates at photovoltaic surface. (iv) The maximum x-coordinate of targeted light spot *P4* is $D_{PVC}/2$, and the minimum x-coordinate of *P4* is zero. If the x-coordinate of spot *P4* is larger than $D_{PVC}/2$, then the part of the reflected sunlight from the above-mirror would be lost instead of reaching the photovoltaic surface. If the x-coordinate of spot *P4* is less than zero, the middle side of the photovoltaics cannot be illuminated. (v) Relative to the sub-mirror, the horizontal shift Wc of the above-mirror needs to be larger than $D_{RC}/2$. If Wc is less than $D_{RC}/2$, the x-coordinate of focus point of above-mirror is also less than $D_{RC}/2$. On the basis of the ray's rectilinear propagation, the x-coordinate of inner spot *P2* of above-mirror would be larger to ensure all the reflected sunlight from above-mirror is cast to photovoltaics. In this case, the photovoltaics would receive a small amount of solar radiation. (vi) The diameter D_{RC} of solar thermochemical reactor should be less than the photovoltaic width D_{PVC}. Otherwise, the aperture width of the above-mirror would be also seriously limited by the thermochemical reactor's radius.

3.2. Maximum possibility of photovoltaic geometric concentration ratio

The photovoltaic geometric concentration ratio $C_{g,PV}$ is defined as the ratio of the aperture width of the above-mirror to the photovoltaic width. The $C_{g,PV}$ is primarily adopted as an indicator for evaluating the

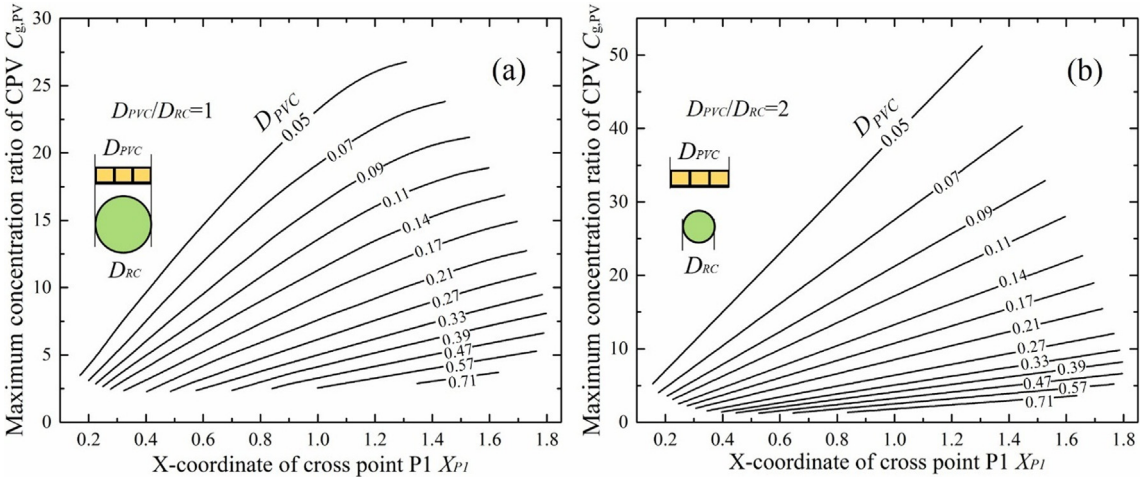

Fig. 3. Variation of maximum photovoltaic geometric concentration ratio $C_{g,PV}$ with x-coordinate X_{P1} of the cross point between mirrors: (a) ratio of photovoltaic width D_{PVC} to diameter D_{RC} of solar thermochemical reactor is 1; (b) ratio of photovoltaic width D_{PVC} to diameter D_{RC} of solar thermochemical reactor is 2.

photovoltaic electricity output in the process of designing the concentrator. As depicted in Fig. 2 at a fixed cross point *P1*, if the x-coordinate of *P4* is $D_{PVC}/2$, then the aperture width of the above-mirror is widest, correspondingly, the value of $C_{g,PV}$ is the largest. Here, according to the Fresnel's law of reflection, the maximum possibility of $C_{g,PV}$ about cross point *P1* is revealed in Fig. 3. It is observed that an increasing variation of $C_{g,PV}$ exists with the rise of x-coordinate x_{p1} of cross point *P1*. The reason for this observation is that a larger value of x_{p1} and a larger width of aperture of the above-mirror correspond to a larger $C_{g,PV}$.

It is noted that the increasing slope of $C_{g,PV}$ with x_{p1} has a difference under the different ratios of D_{PVC} to D_{RC}. For example, when the ratio of D_{PVC} to D_{RC} is set to approximately 1, the increasing slope gradually decreases with the rise of x_{p1}. This behavior can be explained by the shading caused by the thermochemical reactor on the sunlight path from the above-mirror. With the increase of x_{p1}, the x-coordinate of the innermost point *P2* of the above-mirror has a corresponding increase, reducing the rate of the increasing slope of the aperture width of the above-mirror. Namely, there exists a nonlinear variation of $C_{g,PV}$. When this ratio increases to 2, a linear increase of $C_{g,PV}$ comes out with the rise of x_{p1}. It is because that the reflected sunlight of the above-mirror would not be shaded by the thermochemical reactor. In other words, the value of x_{p2} is fixed with the rise of x_{p1}. Furthermore, a linear increase of the aperture width of the above-mirror with x_{p1} results in a linear increase of $C_{g,PV}$ with x_{p1}.

In addition, as shown in Fig. 3, when the ratio of D_{PVC} to D_{RC} approaches 1, the $C_{g,PV}$ could attain approximately 27, and this value can reach up to approximately 50 when the ratio is 2. This means that the maximum possibility of $C_{g,PV}$ can be improved by increasing the ratio of D_{PVC} to D_{RC}. Here, considering the shading effect of the photovoltaics on the incident sunlight, the recommended size ratio is below 2. It means that the splitting concentrator can provide the low-concentration-ratio sunlight for specific photovoltaic materials, such as silicon Si, cadmium telluride CdTe, and organic thin film.

3.3. Solar flux density

In the design of the proposed spectral splitting concentrator, it is needed to consider the uniform illumination over the photovoltaics and solar thermochemical reactor. With the help of the Ray-tracing method, the solar flux distribution can be calculated (see also in Appendix A). Regarding the incident light cone, it is needed to consider the total number *Nc* of sampling points of light cone. For each light cone, the total number *Ns* of incident rays is taken into account. Considering the number N_{loss} of rays not reaching the concentrator, the total number N_{tot} of valid rays is given by $Nc \times Ns\text{-}N_{loss}$. For each valid ray, the carried spectral energy e_k has an attenuation caused by the optical loss in the process of concentrating sunlight. Furthermore, if the received surface of the concentrating photovoltaics is divided into small elements along the width direction, the received solar energy $E_{i,CPV}$ of the photovoltaics can be expressed as

$$E_{i,CPV} = \sum_{k=1}^{N_i} e_{k,PV} = N_i \cdot e_0 \cdot \eta_{opt\_CPV} \tag{5}$$

Similarly, the surface of solar thermochemical reactor is circumferentially divided into small elements. Then, the received solar energy $E_{i,R}$ of thermochemical reactor can be expressed as

$$E_{j,R} = \sum_{k=1}^{N_j} e_{k,R} = e_0 (N_{j\_1}\eta_{opt\_R0} + N_{j\_2}\eta_{opt\_R1} + N_{j\_3}\eta_{opt\_R2}) \tag{6}$$

where i and j are the number of elements of the photovoltaics and the thermochemical reactor, respectively; $_{PV}$ and $_R$ denote the photovoltaics and the thermochemical reactor, respectively; e_0 is the spectral energy carried by the incident ray; η_{opt} is the optical efficiency in the process of concentrating sunlight, which is based on the Ref [36].

In the concentrating solar photovoltaics process, the optical efficiency η_{opt_PV} can be obtained by the multiplication of the above-mirror's clearness and the reflectance, the photovoltaic clearness, the transmittance, the absorptance, the effective length and the intercept factor. In the solar thermochemical process, there are three types of concentrated sunlight that are divided in terms of the times of penetrating through the above-mirror. For each type of concentrated sunlight, the optical efficiency η_{opt_R} can be expressed as

$$\eta_{opt\_R0} = Cl_{sub\_mirror} \cdot \rho_{sub\_mirror} \cdot Cl_{reactor} \cdot \tau_{reactor} \cdot \alpha_{reactor} \cdot L_{reactor\_eff} \cdot \gamma_{reactor} \tag{7}$$

$$\eta_{opt\_R1} = Cl^2_{above\_mirror} \cdot \tau_{above\_mirror} \cdot Cl_{sub\_mirror} \cdot \rho_{sub\_mirror} \cdot Cl_{reactor} \cdot \tau_{reactor} \cdot \alpha_{reactor} \cdot L_{reactor\_eff} \cdot \gamma_{reactor} \tag{8}$$

$$\eta_{opt\_R2} = Cl^4_{above\_mirror} \cdot \tau^2_{above\_mirror} \cdot Cl_{sub\_mirror} \cdot \rho_{sub\_mirror} \cdot Cl_{reactor} \cdot \tau_{reactor} \cdot \alpha_{reactor} \cdot L_{reactor\_eff} \cdot \gamma_{reactor} \tag{9}$$

where *Cl* stands for clearness, ρ is reflectance, τ is transmittance, α is absorptance, *L* is length, γ is intercept factor; the subscripts $_{above\_mirror}$, $_{sub\_mirror}$ and $_{reactor}$ denote above-mirror, sub-mirror and solar thermochemical reactor; the subscript $_{eff}$ is effective. The more details of optical parameters are list in the Appendix A.

Furthermore, to identify the relationship between the solar flux density and the incident irradiation, it needs to determine the relative

solar energy density ξ. In this paper, ξ is defined as the ratio of the solar energy density E/S over the direct normal irradiation DNI. The expressions of the ξ are shown as

$$\xi_{i,PV} = \frac{E_{i,PV}}{S_{i,PV}\cdot DNI} = \frac{f\cdot(A_C - D_{PVC})\cdot\eta_{opt\_PV}}{Ntot\cdot S_{i,PV}} \sum_{k=1}^{N_i} \varsigma\cdot\phi(\beta)_{k,PV} \tag{10}$$

$$\xi_{j,R} = \frac{E_{j,R}}{S_{j,R}\cdot DNI} = \frac{f\cdot(A_C - D_{PVC})}{Ntot\cdot S_{j,R}}\left(\sum_{k=1}^{N_{j\_0}} \varsigma\cdot\phi(\beta)_{k,PV}\cdot\eta_{opt\_R0} + \sum_{k=1}^{N_{j\_1}} \varsigma\cdot\phi(\beta)_{k,PV}\cdot\eta_{opt\_R1} + \sum_{k=1}^{N_{j\_2}} \varsigma\cdot\phi(\beta)_{k,PV}\cdot\eta_{opt\_R2}\right) \tag{11}$$

$$\sum_{i=1}^{N_S} \varsigma\cdot\phi(\beta_i)\frac{1}{N_S} = 1 \tag{12}$$

where $S_{i,PV}$ and $S_{j,R}$ are the area of the micro element on the surface of photovoltaics and the thermochemical reactor at the unit length, respectively. The coefficient ς is a constant.

In addition, the solar radiation can be influenced by atmospheric particulates. With the consideration of such influence, the amount of the spectral energy carried by each incident ray is different in a light cone. This effect is called solar brightness and is described by the distribution function $\phi(\beta)$ [37] that can be expressed as

$$\phi(\beta) = \begin{cases} \frac{\cos(0.326\beta)}{\cos(0.308\beta)}, & \beta \leqslant 4.65 \text{ mrad} \\ e^{k}\beta^{\mu}, & \beta > 4.65 \text{ mrad} \end{cases} \tag{13}$$

where β is the radial angular displacement, $k = 0.9\ln(13.5\chi)\chi^{-0.3}$, $\mu = 2.2\ln(0.52\chi)\chi^{0.43} - 0.1$. In this paper, χ is 6.3%.

4. Design example

4.1. Design parameters and assumptions

Here, the designed spectral splitting concentrator can adopt the state-of-art parabolic trough. The basic data of designed concentrator is shown in Table 1. The sub-mirror has an aperture width of 2550 mm and focus length of 850 mm. As for above-mirror, it consists of two layers of selective film and a law of H-K9L glass. For this film, the theoretical reflectance for the reflected spectrum range is approximately 0.99, and the theoretical transmittance for the remaining spectrum range is approximately 0.98. In addition, a tubular thermochemical reactor is adopted. The covered glass of the reactor has a diameter of 120 mm, and the inner tube of the reactor has a diameter of 38 mm. Moreover, several optical parameters affecting the total optical efficiency are also shown in Table 1, such as clearness, effective length and intercept factor. The other optical parameters dependent on wavelength are described in the Appendix A.

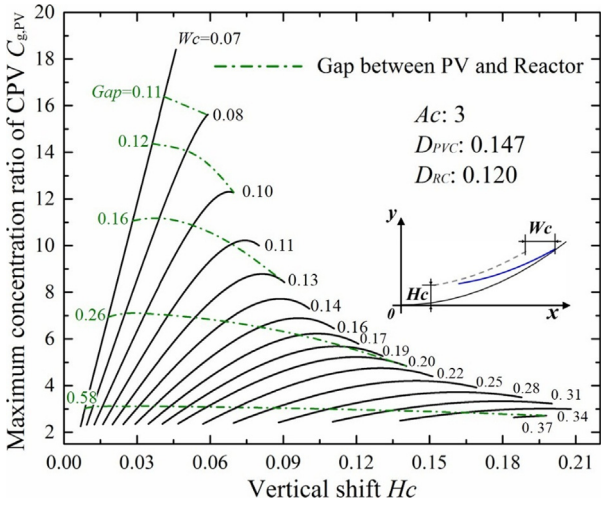

Fig. 4. Variation of the photovoltaic geometric concentration ratio with position relation between above-mirror and sub-mirror. Hc and Wc are vertical shift and horizontal shift of above-mirror to sub-mirror, respectively; Ac is aperture width of sub-mirror, D_{PVC} is photovoltaic width and D_{RC} is diameter of solar thermochemical reactor.

4.2. Position relation between the above-/sub-mirrors

According to Eqs. (17)–(21), we obtain the trace of concentrating sunlight. The shift ranges Wc and Hc of the above-mirror are acquired under the boundary conditions in Section 3.1. Fig. 4 preliminarily illustrates the relative horizontal shift Wc in the range from 0.07 to 0.37 and the relative vertical shift Hc in the range from 0.01 to 0.21. Here, the designed focus length f is set to approximately 850 mm. By multiplying f by the Wc and Hc, the practical horizontal shift W is in the range of 60 mm to 315 mm, and the range of vertical shift H is in the range of from 9 mm to 179 mm. If the value of W or H is not in this range, then the part of the concentrated sunlight directed towards the photovoltaics cannot be intercepted by the photovoltaics. If the value of f is changed, then the values of W and H correspondingly vary. In this case, through the multiplication of the value of f by the values of Wc and Hc presented in Fig. 4, the detailed values of both W and H can be obtained. Therefore, the results in Fig. 4 may provide a guide for designing the geometric relationship between the above-/sub-mirrors.

After determining the ranges of Wc and Hc, we further identify the relationship between the maximum $C_{g,PV}$ and the shift ranges. The presentations in Fig. 4 show that the maximum $C_{g,PV}$ mainly depends on the horizontal shift Wc. For example, when the value of Wc is close to the half width $D_{PVC}/2$ of the photovoltaics, the value of $C_{g,PV}$ can exceed 15. In contrast, when the value of Wc is greater than $D_{PVC}/2$, the $C_{g,PV}$ is limited to below 10. In addition, it can be seen that there exist matches between the relative horizontal shift Wc and the relative vertical shift Hc. In other words, the distribution of solar flux on the photovoltaics

Table 1
The geometric dimensions and optical parameters of the designed spectral splitting concentrator, solar thermochemical reactor, photovoltaics and heat sink.

Items	Values	Items	Values
Spectral splitting concentrator		**Photovoltaics and heat sink**	
Aperture of the sub-mirror A	2550 mm	Width D_{PV}	125 mm
Focus length of the sub-mirror f	850 mm	Thickness of the heat sink	30 mm
Clearness of the above-mirror Cl_{above_mirror}	0.98	Intercept factor γ_{PV}	0.958
Clearness of the sub-mirror Cl_{sub_mirror}	0.98	Effective length L_{PV_eff}	0.92
Solar thermochemical reactor		Clearness of the covered glass Cl_{PV}	0.98
Diameter of the covered glass D_R	102 mm	Photovoltaic absorptance α_{PV}	0.98
Clearness of the covered glass $Cl_{reactor}$	0.98	Emissivity of the covered glass ε_{PV}	0.9
Intercept factor $\gamma_{reactor}$	0.958	Direct normal irradiation DNI	900 W·m^{-2}
Effective length $L_{reactor\_eff}$	0.95	Global horizontal irradiation GHI	1000 W·m^{-2}

can be optimized to be more uniform at a given target of $C_{g,PV}$.

Moreover, it is noted that, the variations in *Wc* and *Hc* also determine the gap between the concentrated photovoltaics and the thermochemical reactor center. In practice, the larger gap is unreasonable, raising a load challenge for the support frames of the photovoltaics and the thermochemical reactor. Thus, this gap would also serve as a key factor to be considered in the design of spectral splitting concentrator. In Fig. 4, it is found that, with the decreases of both *Wc* and *Hc*, the $C_{g,PV}$ is larger and the *Gap* is smaller. In this case, the value of *Wc* is preliminarily selected as 0.07 and 0.08, and the corresponding value of *W* of the above-mirror is determined to be 60 mm and 68 mm, respectively.

4.3. Distribution feature of the solar flux

According to Eqs. (5)–(11), the examination is carried out for the distribution feature of the solar flux over the CPV and the solar thermochemical reactor. Here, the target reflected wavelength range of the above-mirror is selected to be in the range from 500 nm to 1100 nm, according to the band-gap energy level of the monocrystalline silicon photovoltaics M-Si.

***On the concentrating solar photovoltaics*:** Fig. 5a and c present the solar flux distribution on the surface of the CPV. It can be clearly observed that the solar radiation can be uniformly distributed on the photovoltaic surface, except for the photovoltaic surface border. This distribution pattern mainly benefits from the fact that the symmetric above-mirror has an outside shift relative to its optical axis. In this case, the superimposing illumination over the photovoltaics is adjusted to achieve the desired solar flux distribution. This homogenizing sunlight work is conducted in the concentrating sunlight process, in agreement with the reported results [29]. It differs from the addition of a secondary optical element in front of the photovoltaics. The distribution feature mainly depends on the parameters of the concentrator, such as *Wc*.

Fig. 5a and c further compares *Wc* in the range of between 0.07 and 0.08. It is found that a concave variation exists in the middle side of the CPV, when the *Wc* is 0.08 and $C_{g,PV}$ is 15. This is because that at larger value of both $C_{g,PV}$ and *Wc*, a greater amount of solar energy is concentrated on the outer side of photovoltaics rather than on its inner side. Moreover, for a $C_{g,PV}$ smaller than 15, the two distribution features are similar. The illumination on the photovoltaic border is lower than that on the inner position. If this low illumination on the border would impact the CPV performance, mounting a small reflected flat mirror [38] on the photovoltaic border or tailoring the inner side of above-mirror could address this issue. In this manner, the irradiation is concentrated onto the inner side of the CPV rather than onto the border.

***On the solar thermochemical reactor*:** Fig. 5b and d depict the circumferential solar flux distribution of the thermochemical reactor. It is observed that when the *Wc* is 0.07, the solar flux distribution is similar to that in the single solar thermochemical system. The solar illumination is mainly located at the circumferential 120-deg and 240-deg positions of thermochemical reactor, whereas the 180-deg position intercepts a low amount of solar energy [39]. It is noted that such an uneven distribution over the circumferential direction can cause thermal stress concentration of the thermochemical reactor. In contrast, when *Wc* is 0.08, the difference of the solar energy density at the near

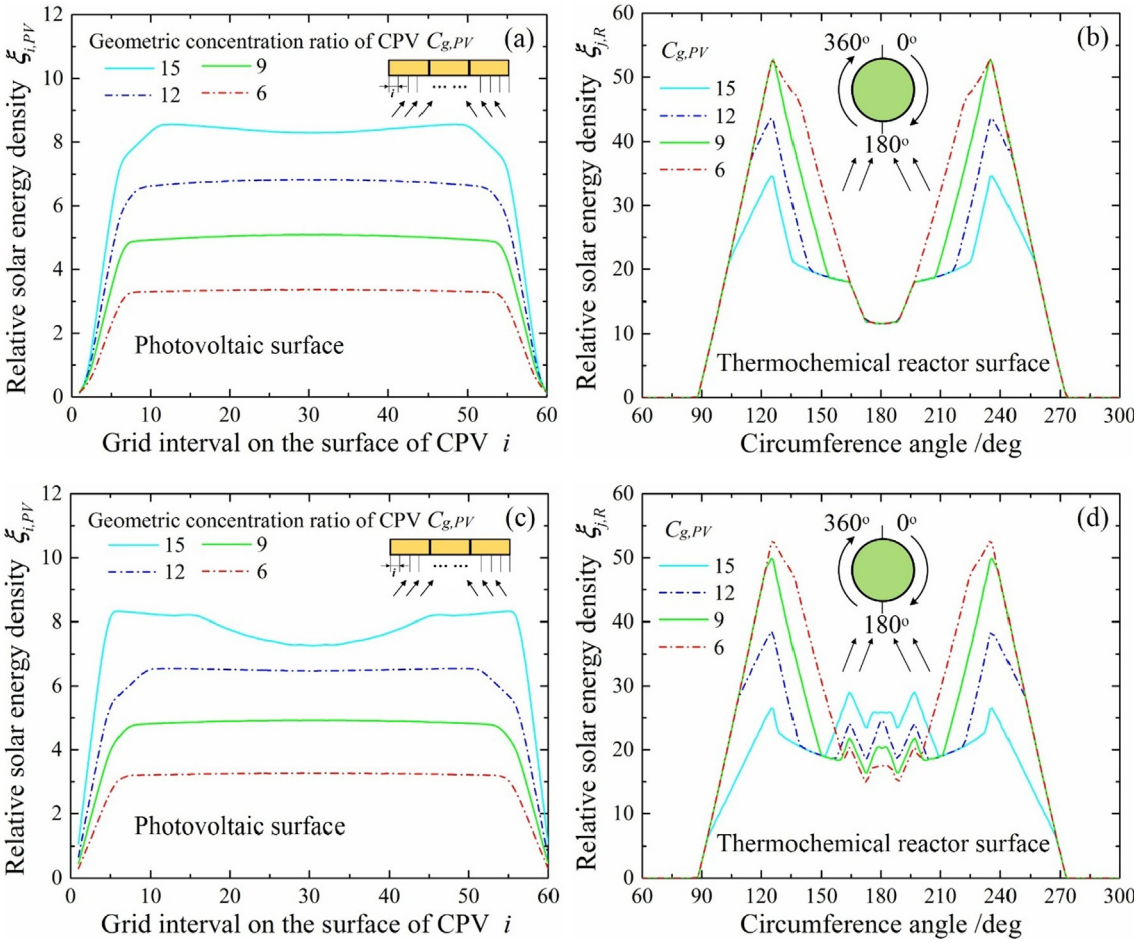

Fig. 5. (a) and (c) are the distribution of solar flux over the photovoltaic surface along its width direction; (b) and (d) are the distribution of solar flux over the solar thermochemical reactor along its circumferential direction. The horizontal shift *Wc* of above-mirror to sub-mirror is 0.07 in (a) and (b), 0.08 in (c) and (d).

and away 180-deg positions is reduced with the gradual increase of $C_{g,PV}$. Obviously, as shown in Fig. 5d, the proposed spectral splitting concentrator can mitigate the thermal stress concentration of thermochemical reactor. Thus, considering this indicator, the final dimension of horizontal shift W is 68 mm, and the range of vertical shift H is from 26 mm to 36 mm.

The basis for the above phenomena is that the Wc can directly influence the attenuation of spectral energy carried by concentrated sunlight reaching the thermochemical reactor. The parabolic trough sub-mirror is divided into two sides by the cross point between above-/sub-mirrors, including the inner side and the outer side. The inner side and the outer side concentrate incident sunlight onto the thermochemical reactor at the near 180-deg position and the away 180-deg position, respectively. When the value of Wc is 0.07, the concentrated sunlight from the inner side of the sub-mirror additionally penetrates through the above-mirror once or twice. In this penetrating process, part of the spectral energy is split and directed towards the CPV via the above-mirror. For this reason, the amount of intercepted solar energy at the near 180-deg position is lower than that of the away 180-deg position. When the value of Wc is 0.08, some concentrated sunlight from the inner side of the sub-mirror would not penetrate through the above-mirror. Thus, for the micro elements over the thermochemical reactor at the near 180-deg position, the received solar energy is higher compared with that of Wc of 0.07. Note that the concentrated sunlight from the outer side of the sub-mirror would penetrate through the above-mirror. In this case, the solar energy density at the away 180-deg position is reduced in contrast to that of Wc at approximately 0.07. Thus, the difference of solar energy density is reduced at the near and away 180-deg positions when Wc is selected as 0.08.

5. Application in a typical solar hybrid system

The spectral splitting concentrator can be introduced into the concentrating solar photovoltaic/ thermochemical hybrid system. Here, the photovoltaics of M-Si and CdTe [40] are employed, the calculation of the photovoltaic generation is based on reference [22]. The methanol decomposition reaction is adopted in the solar thermochemical reactor. The hybrid system converts the solar energy into high-quality photovoltaic electricity $P_{Elec,PV}$ and work-equivalent chemical exergy $Ex_{Sol.}$ carried by solar thermal fuel. And the solar energy conversion efficiency is expressed as

$$\eta_{Sol.} = \frac{P_{Elec,PV} + Ex_{Sol.}}{DNI \cdot A \cdot L_{sub\_mirror}} \tag{14}$$

The details of $P_{Elec,PV}$ and $Ex_{Sol.}$ can be written as

$$P_{Elec,PV} = DNI \cdot C_{g,PV} \cdot D_{PV} \cdot L_{sub\_mirror} \cdot \eta_{opt\_PV} \cdot \eta_{PV} \tag{15}$$

$$Ex_{Sol.} = [DNI \cdot A \cdot L_{sub\_mirror} \cdot \eta_{Sol\_to\_Fuel} + m_{CH3OH} \cdot LHV_{CH3OH}] \cdot 0.87 - m_{CH3OH} \cdot LHV_{CH3OH} \cdot 0.99 \tag{16}$$

where, η_{PV} is the photovoltaic generation efficiency; m_{CH3OH} and LHV_{CH3OH} are the flow rate and the low heating value of the reactive methanol; 0.87 and 0.99 are energy level [41] of solar thermal fuel (mixture of carbon monoxide and hydrogen) and methanol, respectively. The efficiency $\eta_{Sol\_to\_Fuel}$ is a ratio between the total amount of solar energy converted into solar thermal fuel to that of total incident solar energy.

Description of typical hybrid system: Fig. 6 depicts the flow diagram of the hybridization of the concentrating photovoltaic system with the solar-driven methanol decomposition. As an example of M-Si, by the spectral splitting concentrator, the full-spectrum radiation is split into the “solar photovoltaic” radiation (500–1100 nm) and the “solar thermal” radiation (380–500 nm and 1100–4000 nm). This part of “solar photovoltaic” radiation is eventually received by the photovoltaics, and converted into photovoltaic electricity and waste heat. Here, such waste heat is timely dissipated via cooling methanol flowing in the heat sink. In this cooling process, the photovoltaics can be controlled to a suitable operation temperature, and the methanol used as the reactant in the solar thermochemical reactor is preheated. Before flowing into solar thermochemical reactor, this part of the methanol is further heated in the exchanger by absorbing the heat of the mixture leaving from the thermochemical reactor.

In addition, the spectral splitting concentrator casts the “solar thermal” radiation and part of the full-spectrum radiation into the solar thermochemical reactor. This part of solar energy serves as reaction heat that drives the endothermic decomposition reaction of methanol at approximately 200 °C. Subsequently, solar thermal fuel (carbon monoxide and hydrogen) is produced at the methanol conversion rate of 0.99 [42]. Ultimately, the mixture leaving from thermochemical reactor is injected into condenser #2 and separated to be solar thermal fuel and methanol in the separator. The solar thermal fuel is stored for further utilization, and the unreacted methanol is injected into the reactant tank.

Total conversion performance of solar energy: The conversion study of solar energy is conducted under the standard spectrum AM 1.5 spectra, in which the design irradiation DNI is 900 W/m^2. The photovoltaic geometric concentration ratio $C_{g,PV}$ is approximately 9. Table 2 presents the performance of the conversion of solar energy into both electricity and fuel. The solar-to-electricity efficiencies of the M-Si and CdTe are 31.9% and 25.7%, respectively. Compared with the non-concentrating condition, the solar-to-electricity efficiency of the M-Si and CdTe has an absolute enhancement of approximately 11% and 12%, respectively. This enhancement is agreed with that reported in Refs. [43,44]. It means that a greater amount of spectral energy received by CPV is converted into high-grade electricity rather than low-grade waste heat. This situation is a benefit of the spectral splitting approach in the photovoltaic generation process. In addition, individual solar thermochemical system has an efficiency $\eta_{Sol\_to\_Fuel}$ of about 74% which is also agreed with that in Ref. [42]. Thus, the validation of performance analysis can be guaranteed.

For the example of a commercial CdTe working at 400–850 nm, the hybrid system produces high-grade electricity of approximately 138 W and chemical exergy rate of approximately 299 W. The total conversion efficiency is approximately 19.0%. Compared with single CPV system, approximately 5.9% absolute enhancement of high-grade conversion efficiency is realized. This improvement benefits from the proposed concentrator casts solar radiation that is unsuitable for photovoltaic power generation to the thermochemical reactor for driving the reaction. Moreover, in contrast to a single solar thermochemical system, the visible radiation is split from the full-spectrum radiation and concentrated to CPV to directly generate electricity. It would be approximately 5.5% absolute enhancement of high-grade conversion efficiency. Thus, the spectral splitting concentrator would offer the possibility to match the conversion of solar energy with the appropriate energy band. The irreversible loss is expected to be reduced in the solar photovoltaic and solar thermochemical processes. The results indicate that the proposed spectral splitting concentrator may realize the cascading utilization of the full-spectrum solar energy.

6. Summary and outlook

Nowadays, the implement of spectral splitting hybrid system is expected to further reduce the cost of solar energy utilization by converting solar energy into high-quality energy. This paper proposes a concentrating solar photovoltaic/thermochemical hybrid system, and a spectral splitting parabolic trough concentrator having an above-mirror and a sub-mirror is designed. The hybrid system converts incident solar radiation into electricity and solar thermal fuel. For clearly revealing the improvement of solar energy utilization, the amount of produced solar thermal fuel should be counted as output of electricity. Here, an electric efficiency 39.4% of internal combustion engine is considered

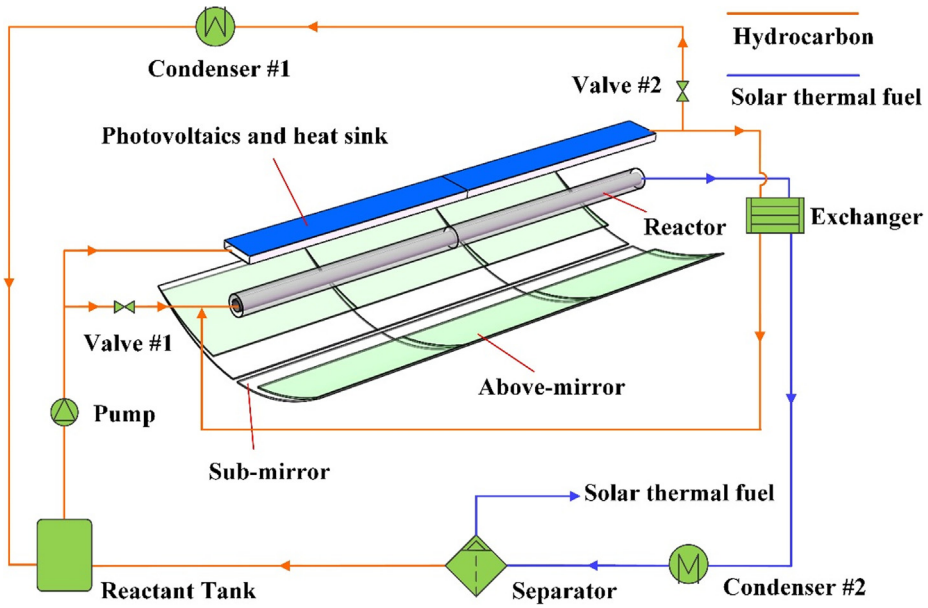

Fig. 6. Flow diagram of hybrid system: partial of solar radiation is cast to photovoltaics for generating electricity, and rest solar radiation is used to drive hydrocarbon decomposition and converted into solar thermal fuel.

Table 2
Performance and improvement of solar energy utilization in the hybrid system (per meter long of concentrator).

Parameters	Values	
	M-Si	CdTe
Hybrid system		
Incident solar radiation	2295 W	2295 W
Photovoltaic electricity	185.9 W	137.6 W
Flow rate of the solar thermal fuel	118 mol/hr	121 mol/hr
Chemical exergy rate provided by solar energy	291.4 W	299.4 W
Photovoltaic electricity and chemical exergy rate	477.3 W	437.0 W
PV efficiency at concentrating condition	31.9%	25.7%
PV efficiency at non-concentrating condition	21.1%	13.9%
Total optical efficiency of hybrid system	76.5%	76.4%
Solar energy conversion efficiency	20.8%	19.0%
Single concentrating photovoltaic system with the same geometric concentration ratio		
Total optical efficiency of single system	75.4%	75.4%
Photovoltaic electricity	198.2 W	136.2 W
Solar energy conversion efficiency	19.6%	13.1%
Absolute enhancement of efficiency in hybrid system	1.2%	5.9%
Single thermochemical system with the same aperture width of the sub-mirror		
The efficiency $\eta_{Sol\_to\_Fuel}$	73.6%	73.6%
Chemical exergy rate provided by solar energy	310.1 W	310.1 W
Solar energy conversion efficiency	13.5%	13.5%
Absolute enhancement of efficiency in hybrid system	7.3%	5.5%

[42]. The solar-to-electricity efficiency of described hybrid system could reach to about 32.0% and 30.6%, respectively, when the M-Si and CdTe are employed. Under the 900 W/m^2 irradiation, mirror area estimated (above-/sub-mirrors) corresponding to per-kilowatt electricity is about 5.0 m^2/kW and 5.2 m^2/kW. Meanwhile, the individual concentrating photovoltaic system has the solar-to-electricity efficiency of 19.6% (using M-Si) and 13.1% (using CdTe), the mirror area would be estimated as about 5.7 m^2/kW and 8.5 m^2/kW. This indicates that the mirror area can be reduced by 12% to 40% in the hybrid system compared to that in the individual system. As is well known, the costs of investment, operation and maintenance restrict the commercial application of solar energy. In this case, using the proposal, the reduction of mirror area by 10% to 40% can provide the possibility of realizing cost-effective solar energy utilization.

Besides, it is well known that solar energy has space-time intermittency. For this reason, regarding high-latitude area, the solar energy is commonly redundant in summer and insufficient in winter for realizing stable power supply in the solar power plant. As such, the average solar efficiency is poor. The hybrid system would be expected to improve average efficiency in the solar energy utilization. For example, the redundant solar energy can be stored via the storage of the solar thermal fuel in summer. On the contrary, the stored solar chemical energy could be released when solar radiation is absent in winter. Meanwhile, the proposed hybrid system is also able to balance the difference of solar radiation between daytime and nighttime. Lastly, the hybrid system presented in our manuscript is easily applied in both small-scale and large-scale scenarios (e.g., household equipment and smart grid [45]) to synchronously provide electricity and solar thermal fuel.

7. Conclusions

A spectral splitting concentrator was proposed and designed for the achievement of cascading utilization of the full-spectrum solar energy. It can selectively concentrate solar radiation to the solar photovoltaic process and solar thermochemical process. Moreover, the proposed concentrator can also provide uniform illumination for concentrating photovoltaics and solar thermochemical reactor. A design methodology was given. Furthermore, a design example was considered to examine the feasibility of proposed concentrator. The results of the design example indicated that the irradiance profile over the photovoltaics was uniform. The use of this uniform irradiance profile can ensure the current match among the photovoltaics connected in series under the concentrating condition. The proposed spectral splitting concentrator also moderated the local Gaussian distribution on the thermochemical reactor in the conventional thermochemical process. Compared with the addition of the secondary optical element, the proposed spectral splitting concentrator can overcome the problem of chromatic aberration while realizing the uniform distribution of solar flux. By integrating

the spectral splitting concentrator and concentrating solar photovoltaic/thermochemical hybrid system, the total conversion efficiency of both solar-to-electricity and solar-to-fuel achieved was 19.0%, 5.9 points higher than that in the individual concentrating photovoltaic system.

Acknowledgments

The authors gratefully acknowledge the support of the National Natural Science Foundation of China (Grant No. 51590904) and the key research program of the Chinese Academy of Sciences (Grant No. KFZD-SW-418).

Appendix A

***Incident ray and reflection ray*:** The incident light cone is considered in two dimensions. Here, the direction vectors of the incident ray and the reflected ray are assumed as (a, b) and (c, d), respectively. At a given an incident point $P5(x_{p5}, y_{p5})$on the concentrator, according to the law of reflection, the relationship between direction vectors are expressed as

$$c = a - \frac{a\cdot\alpha^2 - 2b\cdot\alpha}{2\beta^2} \tag{17}$$

$$d = b + \frac{a\cdot\alpha - 2b}{\beta^2} \tag{18}$$

where $\alpha = x_{P5} - Wcc$, and $\beta = \sqrt{\alpha^2/4 + 1}$. For the above-mirror, when x_{p5} is greater than 0, $Wcc = Wc$; otherwise, $Wcc = -Wc$. For the sub-mirror, $Wcc = 0$ and $Hc = 0$.

Correspondingly, the equation of reflected ray $Ax + By + C = 0$ can be obtained, in which the coefficients are

$$A = -b + \frac{2b - a\cdot\alpha}{\beta^2} \tag{19}$$

$$B = a - \frac{a\cdot\alpha^2 - 2b\cdot\alpha}{2\beta^2} \tag{20}$$

$$C = \frac{a}{8\beta^2}\alpha^4 - \frac{b}{4\beta^2}\alpha^3 + \left(\frac{2a + a\cdot Hc}{2\beta^2} - \frac{a}{4}\right)\alpha^2 + \left(b + \frac{a\cdot Wc - 2b - b\cdot Hc}{\beta^2}\right)\alpha + \left(b\cdot Wc - \frac{2b\cdot Wc}{\beta^2} - a\cdot Hc\right) \tag{21}$$

***Calculation grid*:** As depicted in Fig. 7, the solar disk grid is built for presenting the uniform distribution of incident rays inside each light cone. The concentrator aperture grid is established for showing the uniform distribution of sampling points of light cones on the both sides of the photovoltaics. The number N_{tot} of valid rays that are concentrated on the photovoltaics and the thermochemical reactor is calculated; these rays indicate the total solar energy collected by the concentrator. The spectral energy e_o for each incident ray is expressed as

$$e_0 = \frac{DNI\cdot f\cdot(Ac - D_{PVC})}{Ntot} \tag{22}$$

***Optical parameter*:** As shown in Fig. 8, the presentations of optical parameters include the reflectance of the sub-mirror [46] and selective coating of solar thermochemical reactor [47], the transmittance [48] of the covered glass of photovoltaics and solar thermochemical reactor (high borosilicate glass), the transmittance [49] of H-K9L glass (base material of above-mirror).

***Refractor*:** Fig. 9 presents some common types of refractor including kaleidoscope, half egg and compound form. The refractor is used as secondary optical element in the front of photovoltaics to homogenize sunlight. In the homogenizing sunlight process, the concentrated sunlight is bended many times when it penetrates through refractor. As a result, the concentrated sunlight can uniformly illuminate over the photovoltaics.

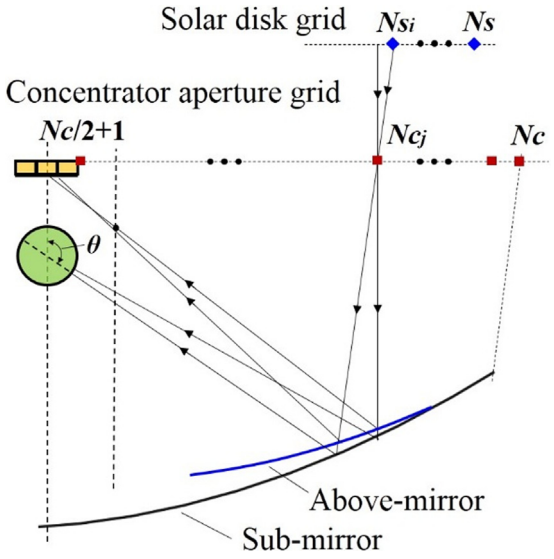

Fig. 7. Schematic diagram of the calculation grid on the one side of spectral splitting concentrator: solar disk grid depicts the uniform distribution of incident rays inside each light cone; concentrator aperture grid shows the uniform distribution of light cone along aperture direction of concentrator.

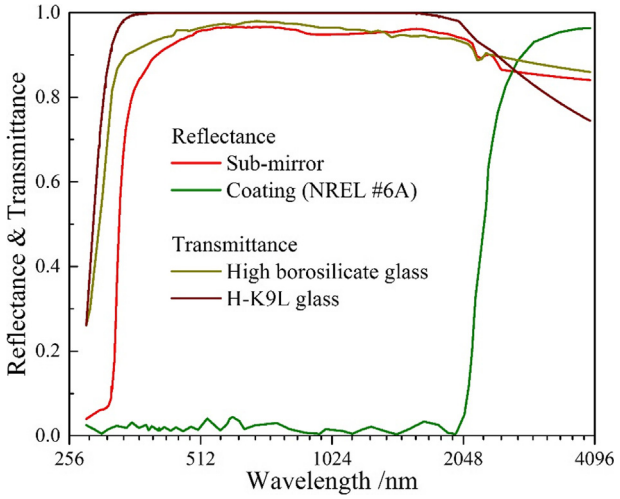

Fig. 8. Reflectance parameters of sub-mirror and reactor's coating; transmittance parameters of covered glasses (photovoltaics and reactor) and basic glass of above-mirror.

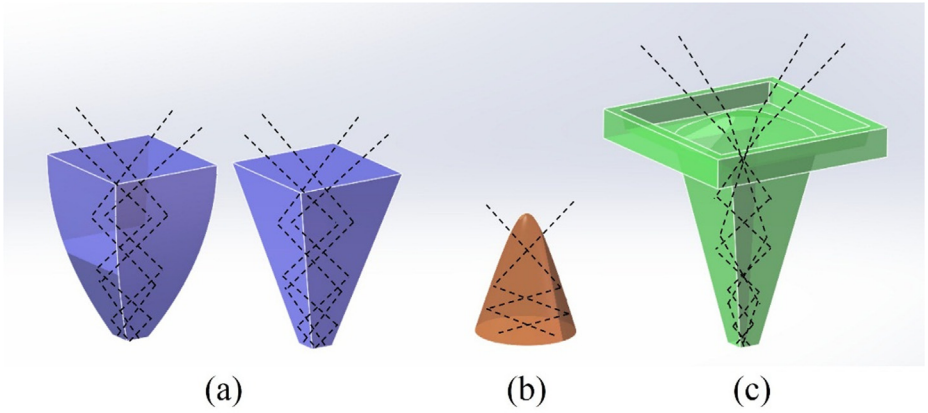

Fig. 9. Secondary optical elements (refractor): (a) molded kaleidoscope with compound parabolic concentrator shaped or flat walls; (b) small half-egg; (c) compound forms.

References:

[1] Philibert Cédric. International energy agency. Renewable energy: solar energy perspectives. IEA; 2011.
[2] Bermel P, Yazawa K, Gray JL, et al. Hybrid strategies and technologies for full spectrum solar conversion. Energy Environ Sci 2016;9:2776–88.
[3] Mojiri Ahmad, Taylor Robert, Thomsen Elizabeth, et al. Spectral beam splitting for efficient conversion of solar energy—a review. Renew Sustain Energy Rev 2013;28:654–63.
[4] Islam Kazi, Riggs Brian, Jia Yaping, et al. Transmissive microfluidic active cooling for concentrator photovoltaics. Appl Energy 2019;236:906–15.
[5] US Department of energy. Advanced research projects agency-energy annual report for FY2013; 2013.
[6] Bisquert Juan. The physics of solar cells: perovskites, organics, and photovoltaic fundamentals. Taylor & Francis Group; 2018.
[7] Renno Carlo. Optimization of a concentrating photovoltaic thermal (CPV/T) system used for a domestic application. Appl Therm Eng 2014;67:396–408.
[8] Coventry Joe S. Performance of a concentrating photovoltaic/thermal solar collector. Sol Energy 2005;78:211–22.
[9] Tourkov Konstantin, Schaefer Laura. Performance evaluation of a PVT/ORC (photovoltaic thermal/organic Rankine cycle) system with optimization of the ORC and evaluation of several PV (photovoltaic) materials. Energy 2015;82:839–49.
[10] Rahbar Kiyarash, Riasi Alireza. Heat recovery of nano-fluid based concentrating Photovoltaic Thermal (CPV/T) Collector with Organic Rankine Cycle. Energy Convers Manage 2019;179:373–96.
[11] Xing Ju, Chao Xu, Han Xue, et al. A review of the concentrated photovoltaic/thermal (CPVT) hybrid solar systems based on the spectral beam splitting technology. Appl Energy 2017;187:534–63.
[12] Imenes AG, Mills DR. Spectral beam splitting technology for increased conversion efficiency in solar concentrating systems: a review. Sol Energy Mater Sol Cells 2004;84:19–69.
[13] Ulavi Tejas U, Davidson Jane H, Hebrink Tim. Analysis of a hybrid PV/T concept based on wavelength selective mirror films. J Sol Energy Eng 2014;136:031009.
[14] Jiang Shouli, Hu Peng, Mo Songping, et al. Optical modeling for a two-stage parabolic trough concentrating photovoltaic/thermal system using spectral beam splitting technology. Sol Energy Mater Sol Cells 2010;94:1686–96.
[15] Segal Akiba, Epstein Michael, Yogev Amnon. Hybrid concentrated photovoltaic and thermal power conversion at different spectral bands. Sol Energy 2004;76:591–601.
[16] Apostoleris Harry, Stefancich Marco, Chiesa Matteo. Concentrating photovoltaics (CPV): the path ahead. Springer International Publishing; 2018.
[17] Connolly John S. Photochemical conversion and storage of solar energy. Elsevier Inc.; 1981.
[18] Romero Manuel, Steinfeld Aldo. Concentrating solar thermal power and thermochemical fuels. Energy Environ Sci 2012;5:9234–45.
[19] Bicer Yusuf, Sprotte André Felipe Vitorio, Dincer Ibrahim. Concentrated solar light splitting using cold mirrors for photovoltaics and photonic hydrogen production applications. Appl Energy 2017;197:169–82.
[20] Sun Jie, Wang Ruilin, Hong Hui, et al. An optimized tracking strategy for small-scale double-axis parabolic trough collector. Appl Therm Eng 2017;112:1408–20.
[21] Li Wenjia, Wang Hongsheng, Hao Yong. A PVTC system integrating photon-enhanced thermionic emission and methane reforming for efficient solar power generation. Sci Bull 2017;62(20):1380–7.
[22] Wanjun Qu, Hong Hui, Li Qiang, et al. Co-producing electricity and solar syngas by transmitting photovoltaics and solar thermochemical process. Appl Energy 2018;217:303–13.
[23] Baig Hasan, Heasman Keith C, Mallick Tapas K. Non-uniform illumination in concentrating solar cells. Renew Sustain Energy Rev 2012;16(8):5890–909.
[24] Abdelhamid Mahmoud, Widyolar Bennett K, Jiang Lun, et al. Novel double-stage high-concentrated solar hybrid photovoltaic/thermal (PV/T) collector with non-imaging optics and GaAs solar cells reflector. Appl Energy 2016;182:68–79.
[25] Renzi Massimiliano, Cioccolanti Luca, Barazza Giorgio, et al. Design and experimental test of refractive secondary optics on the electrical performance of a 3-junction cell used in CPV systems. Appl Energy 2017;185:233–43.

[26] Algora C, Rey-Stolle I. Handbook on concentrator photovoltaic technology. Wiley; 2016.
[27] Chong Kok-Keong, Lau Sing-Liong, Yew Tiong-Keat, et al. Design and development in optics of concentrator photovoltaic system. Renew Sustain Energy Rev 2013;19:598–612.
[28] Shanks Katie, Senthilarasu S, Mallick Tapas K. Optics for concentrating photovoltaics: trends, limits and opportunities for materials and design. Renew Sustain Energy Rev 2016;60:394–407.
[29] Bader R, Steinfeld A. Solar trough concentrator design for uniform radiative flux distribution. Opt Solar Energy 2014.
[30] Nilsson Johan, Leutz Ralf, Karlssona Björn. Micro-structured reflector surfaces for a stationary asymmetric parabolic solar concentrator. Sol Energy Mater Sol Cells 2007;91:525–33.
[31] Zhuang Zhenfeng, Feihong Yu. Optimization design of hybrid Fresnel-based concentrator for generating uniformity irradiance with the broad solar spectrum. Opt Laser Technol 2014;60:27–33.
[32] Tan Ming-Hui, Chong Kok-Keong, Wong Chee-Woon. Optical characterization of nonimaging dish concentrator for the application of dense-array concentrator photovoltaic system. Appl Opt 2014;53(3):475–86.
[33] Schmitz Max, Dähler Fabian, Elvinger Francois, et al. Nonimaging polygonal mirrors achieving uniform irradiance distributions on concentrating photovoltaic cells. Appl Opt 2017;56(11):3035–52.
[34] Perez-Enciso Ricardo, Gallo Alessandro, Riveros-Rosas David, et al. A simple method to achieve a uniform flux distribution in a multifaceted point focus concentrator. Renew Energy 2016;93:115–24.
[35] Liu Yang, Peng Hu, Zhang Qian, et al. Thermodynamic and optical analysis for a CPV/T hybrid system with beam splitter and fully tracked linear Fresnel reflector concentrator utilizing sloped panels. Sol Energy 2014;103:191–9.
[36] Valenzuela Loreto, López-Martín Rafael, Zarza Eduardo. Optical and thermal performance of large-size parabolic-trough solar collectors from outdoor experiments: a test method and a case study. Energy 2014;70:456–64.
[37] Buie D, Monger AG, Dey CJ. Sunshape distributions for terrestrial solar simulations. Sol Energy 2003;74(2):113–22.
[38] Zhang Heng, Chen Haiping, Han Yuchen, et al. Experimental and simulation studies on a novel compound parabolic concentrator. Renew Energy 2017;113:784–94.
[39] Cheng ZD, He YL, Xiao J, et al. Three-dimensional numerical study of heat transfer characteristics in the receiver tube of parabolic trough solar collector. Int Commun Heat Mass Transf 2010;37:782–7.
[40] Amanlou Y, Hashjin TT, Ghobadian B, et al. A comprehensive review of uniform solar illumination at low concentration photovoltaic (LCPV) systems. Renew Sustain Energy Rev 2016;60:1430–41.
[41] Ishida M. Thermodynamics made comprehensible. New York: Nova Science Publishers, Inc.; 2002.
[42] Bai Zhang, Liu Qibin, Lei Jing, et al. Investigation on the mid-temperature solar thermochemical power generation system with methanol decomposition. Appl Energy 2018;217:56–65.
[43] Crisostomo Felipe, Taylor Robert A, Zhang Tian, et al. Experimental testing of SiNx/SiO2 thin film filters for a concentrating solar hybrid PV/T collector. Renew Energy 2014;72:79–87.
[44] Widyolar Bennett, Jiang Lun, Winston Roland. Spectral beam splitting in hybrid PV/T parabolic trough systems for power generationn. Appl Energy 2018;209:236–50.
[45] O'Dwyer Edward, Pan Indranil, Acha Salvador, Shah Nilay. Smart energy systems for sustainable smart cities: current developments, trends and future directions. Appl Energy 2019;237:581–97.
[46] Good Philipp, Cooper Thomas, Querci Marco, et al. Spectral reflectance, transmittance, and angular scattering of materials for solar concentrators. Sol Energy Mater Sol Cells 2016;144:509–22.
[47] Kennedy Cheryl. Hank Price. Progress toward developing a durable high-temperature solar selective coating. National Renewable Energy Laboratory; 2007.
[48] Navarro-Hermoso JL, Espinosa-Rueda G, Heras C, et al. Parabolic trough solar receivers characterization using specific test bench for transmittance, absorptance and heat loss simultaneous measurement. Sol Energy 2016;136:268–77.
[49] Optical glass. Hubei New Huaguang Information Materials CO., LTD, China; 2017.